ICIEM 2021

14TH INTERNATIONAL CONGRESS OF
INBORN ERRORS OF METABOLISM

21-23 NOVEMBER 2021, SYDNEY, AUSTRALIA

A knock-in rat model unravels acute and chronic renal toxicity in glutaric aciduria type I

Mary Gonzalez Melo[1], Andrea Fontana[2], David Viertl[2], Gilles Allenbach[2], John O. Prior[2], Samuel Rotman[3], René Günther Feichtinger[4], Johannes Adalbert Mayr[4], Michele Costanzo[5,6], Marianna Caterino[5,6], Margherita Ruoppolo[5,6], Olivier Braissant[7], Frederic Barbey[8], Diana Ballhausen[1]

[1]Pediatric Metabolic Unit, Pediatrics, Woman-Mother-Child Department, University of Lausanne and University Hospital of Lausanne, Switzerland
[2]Department of Nuclear Medicine and Molecular Imaging, University of Lausanne and Lausanne University Hospital, Lausanne, Switzerland
[3]Service of Clinical Pathology, University of Lausanne and University Hospital of Lausanne, Switzerland
[4]Department of Pediatrics, University Hospital Salzburg, Paracelsus Medical University, Salzburg Austria.
[5]Department of Molecular Medicine and Medical Biotechnology, School of Medicine, University of Naples Federico II, 80131 Naples, Italy
[6]CEINGE – Biotecnologie Avanzate s.c.ar.l., 80145 Naples, Italy
[7]Service of Clinical Chemistry, University of Lausanne and University Hospital of Lausanne, Switzerland
[8] Department of immunology, University of Lausanne and University Hospital of Lausanne, Switzerland

Background

Glutaric aciduria type I (GA-I, OMIM # 231670) is an autosomal recessive inborn error of metabolism caused by deficiency of the mitochondrial enzyme glutaryl-CoA dehydrogenase (GCDH). The principal clinical manifestation in GA-I patients is striatal injury most often triggered by catabolic stress. Early diagnosis by newborn screening programs improved survival and reduced striatal damage in GA-I patients. However, the clinical phenotype is still evolving in the aging patient population. Evaluation of long-term outcome in GA-I patients recently identified glomerular filtration rate (GFR) decline with increasing age. We recently created the first knock-in rat model for GA-I harboring the mutation p.R411W (c.1231 C>T), corresponding to the most frequent *GCDH* human mutation p.R402W.

Objectives

To examine:

- the effect of an acute metabolic stress in form of high lysine diet (HLD) on young *Gcdh*$^{ki/ki}$ rats
- the chronic effect of GCDH deficiency on kidney function in a longitudinal study on a cohort of *Gcdh*$^{ki/ki}$ rats

ICIEM 2021

14TH INTERNATIONAL CONGRESS OF
INBORN ERRORS OF METABOLISM

21-23 NOVEMBER 2021, SYDNEY, AUSTRALIA

Methods

Design for the study of acute renal toxicity in GA-I

4 WT and 4 KI rats under high lysine diet (HLD)
4 WT and 4 KI rats under normal diet (ND)
Total number of animals: 16

Animal evaluation 2x/d (score sheet),
constant supervision of rats by web camera

D= Days
W= Weeks

ND: 1.1% L-lysine
HLD: 4.7% L-lysine

Rat Age	W-3	W-6	
Time of diet	W-0 D-0	W-3 D-21	
Linked Interventions		-Sublingual blood harvest -Urine harvest -Isoflurane anesthesia -Radiotracer injection -Obtaining image **-Sacrifice**	

Design for the study of chronic renal toxicity in GA-I

	childhood	adolescence	young adult	adulthood	elderly
Rat Age	W-3	W-6	M-3	M-6	M-12
Intervention micropet No	1	2	3	4	5
Linked Interventions	-Isoflurane anesthesia -Radiotracer injection -Obtaining image	-Isoflurane anesthesia -Radiotracer injection -Obtaining image	-Isoflurane anesthesia -Radiotracer injection -Obtaining image	-Isoflurane anesthesia -Radiotracer injection -Obtaining image	-Isoflurane anesthesia -Radiotracer injection -Obtaining image **-Sacrifice**

W= Weeks
M= Months

WT rats: 5 females + 5 males
KI rats: 5 females + 5 males
Total number of animals: 20

Results 1

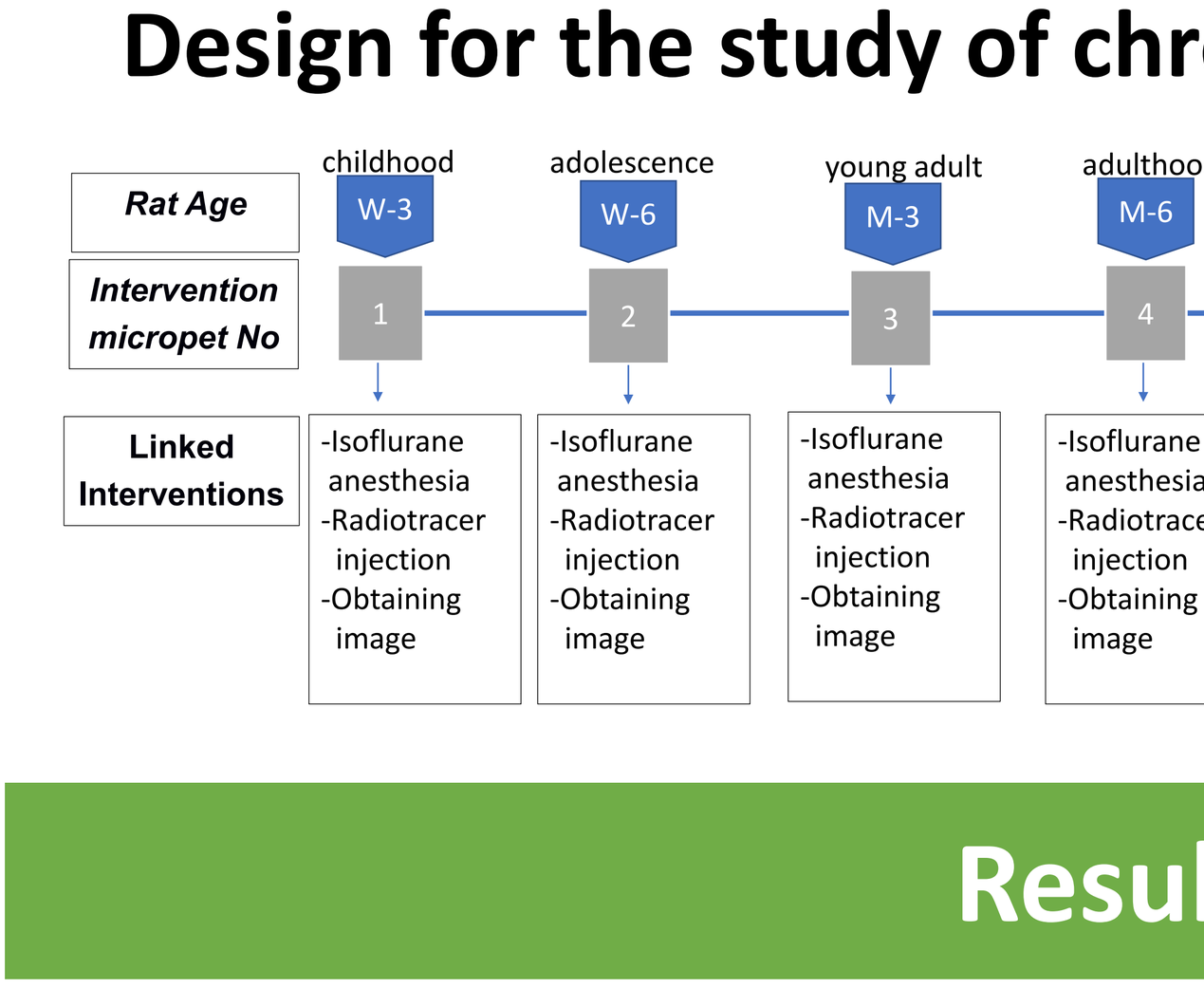

Figure 1. Decreased GFR in 6-week-old *Gcdh*$^{ki/ki}$ rats under HLD and progressive GFR decline in aging *Gcdh*$^{ki/ki}$ rats under ND. WT and *Gcdh*$^{ki/ki}$ rats at the age of 6 weeks fed since 21 days with either ND or HLD and WT and *Gcdh*$^{ki/ki}$ rats under ND at 6 weeks, 3, 6 and 12 months of age were investigated by micro-PET/CT imaging with injection of the radiotracer ^{68}Ga-EDTA. Dynamic reconstruction was obtained using software PMOD 3.7. Glomerular filtration rate (GFR) (**A and F**), renal volume (**B and G**) and renal clearance (CLren) (**C and H**) were calculated as described in the material and methods section. GFR was found to be significantly decreased in *Gcdh*$^{ki/ki}$ rats under HLD (**A**). Renal volume (**B**) and CLren (**C**) did not show any significant differences, but tended to decrease in *Gcdh*$^{ki/ki}$ rats under HLD. After dissection, kidney weight (**D**) and length (**E**) were measured. Kidney weight was significantly higher in *Gcdh*$^{ki/ki}$ rats under ND, but significantly lower under HLD as compared to WT rats under the same diet. (**D**). Kidney length was found significantly reduced in *Gcdh*$^{ki/ki}$ rats under HLD (**E**). A significant decrease of GFR was observed in *Gcdh*$^{ki/ki}$ rats under ND at the age of 3 months (**F**). Renal volumes did not vary significantly between WT and *Gcdh*$^{ki/ki}$ rats under ND (**G**). CLren decreased significantly in *Gcdh*$^{ki/ki}$ rats under ND after 6 months (H). Results of WT are indicated in white, results of *Gcdh*$^{ki/ki}$ rats in grey. Data shown as mean ± SD; Tukey test or Mann Whitney after ANOVA two ways analysis or Kruskal Wallis for cross sectional analysis and Student's t-test or Mann Whitney test for longitudinal cohort analysis: *$p < 0.05$, **$p = 0.01$ ***$p = 0.001$ and ****$p < .0001$. Min. n=3 for all conditions.

CHUV

UNIL | Université de Lausanne

ICIEM 2021

14TH INTERNATIONAL CONGRESS OF
INBORN ERRORS OF METABOLISM

21-23 NOVEMBER 2021, SYDNEY, AUSTRALIA

Results 2

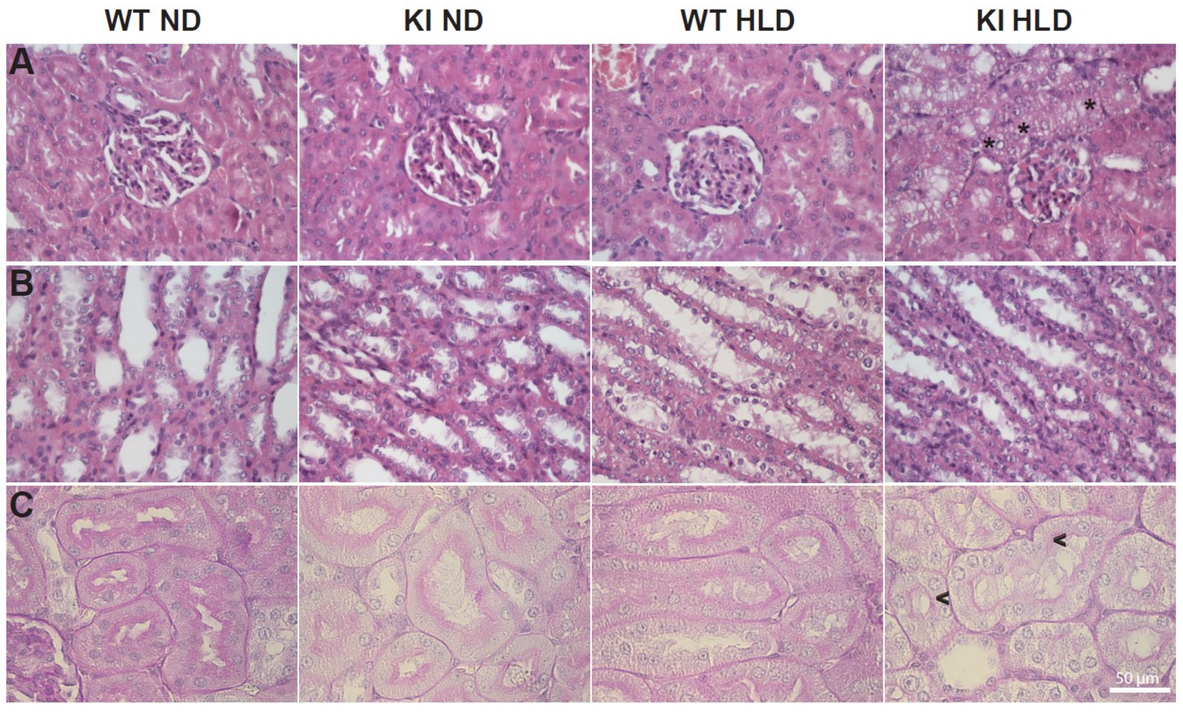

Figure 2. Vacuoles and brush border membrane thinning in 6-week-old *Gcdh*$^{ki/ki}$ rats under HLD. Light micrographs of representative HE (**A and B**) and PAS (**C**) stained paraffin sections (4 µm) of kidneys from 6-week-old WT and *Gcdh*$^{ki/ki}$ rats under ND and HLD. Vacuoles (**asterisks**) were detected in PT cells of *Gcdh*$^{ki/ki}$ rats under HLD (**A**). Glomeruli (**A**) and distal tubules (**B**) did not show any significant differences between WT and *Gcdh*$^{ki/ki}$ rats under ND and HLD. PAS staining revealed thinning of brush border membrane in *Gcdh*$^{ki/ki}$ rats under HLD (**arrows**) (**C**). Scale bar 50 µm. Min. n=4 for all conditions.

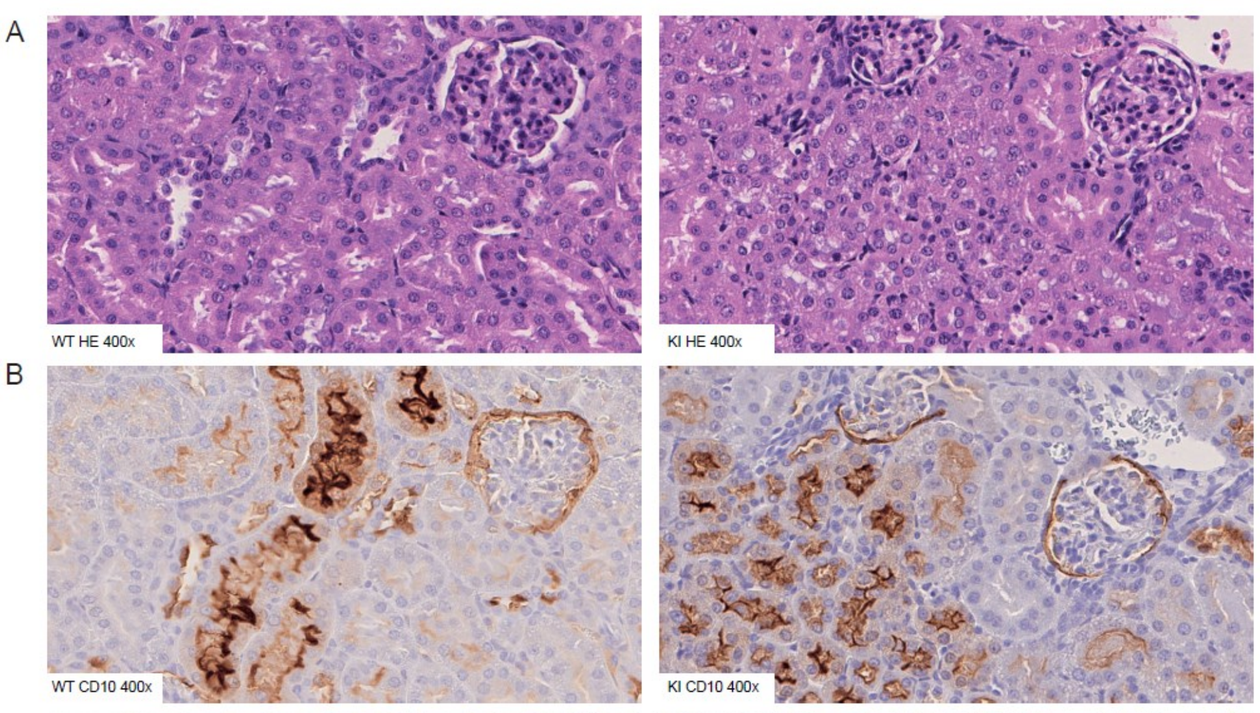

Figure 3. Vacuoles are localized in renal PT cells of 6-week-old *Gcdh*$^{ki/ki}$ rats under HLD and have a lipophilic content. (**A**) HE staining on sagittal kidney sections of 6-week-old WT (**left**) and *Gcdh*$^{ki/ki}$ (KI) (**right**) rats under HLD. (**B**) Immunostaining for CD10 on sagittal kidney sections of 6-week-old WT (**left**) and *Gcdh*$^{ki/ki}$ (KI) (**right**) rats under HLD confirmed localization of vacuoles in PT cells. (**C**) Oil Red O staining on sagittal kidney sections of 6-week-old WT (**left**) and *Gcdh*$^{ki/ki}$ (KI) (**right**) rats revealed a lipophilic content of vacuoles in *Gcdh*$^{ki/ki}$ (KI) under HLD. Scale bar 50 µM. Min. n=4 for all conditions.

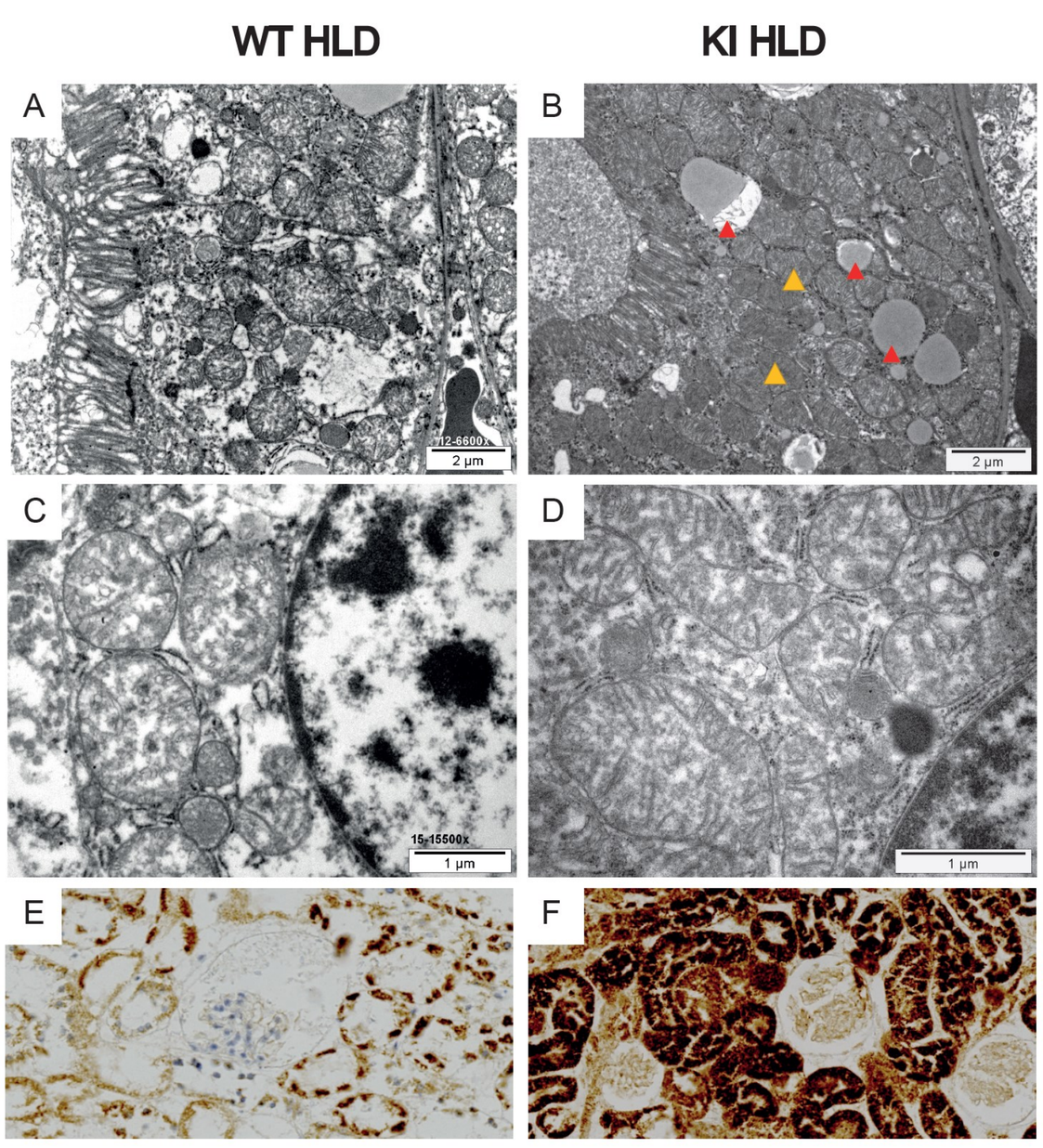

Figure 4. Vacuoles and increased numbers of mitochondria in renal PT cells of 6-week-old *Gcdh*$^{ki/ki}$ rats under HLD. Results from 6-week-old WT (**left column, A, C, E**) and *Gcdh*$^{ki/ki}$ rats (**right column, B, D, F**) under HLD. Transmission electron microscopy (**A-D**) revealed vacuoles (**red triangles**) and an increased number of enlarged mitochondria (**yellow triangles**) in the cytosol of renal PT cells in *Gcdh*$^{ki/ki}$ rats under HLD (**B, D**). Immunohistochemical staining for VDAC1 was significantly increased in *Gcdh*$^{ki/ki}$ renal PT cells (**F**) compared to WT PT cells (**E**). Scale bars A and B 2 µm, C and D 1 µm, E and F 50 µm. (**G**) Increased citrate synthase enzymatic activity in *Gcdh*$^{ki/ki}$ rats under HLD. Min. n=4 for all conditions.

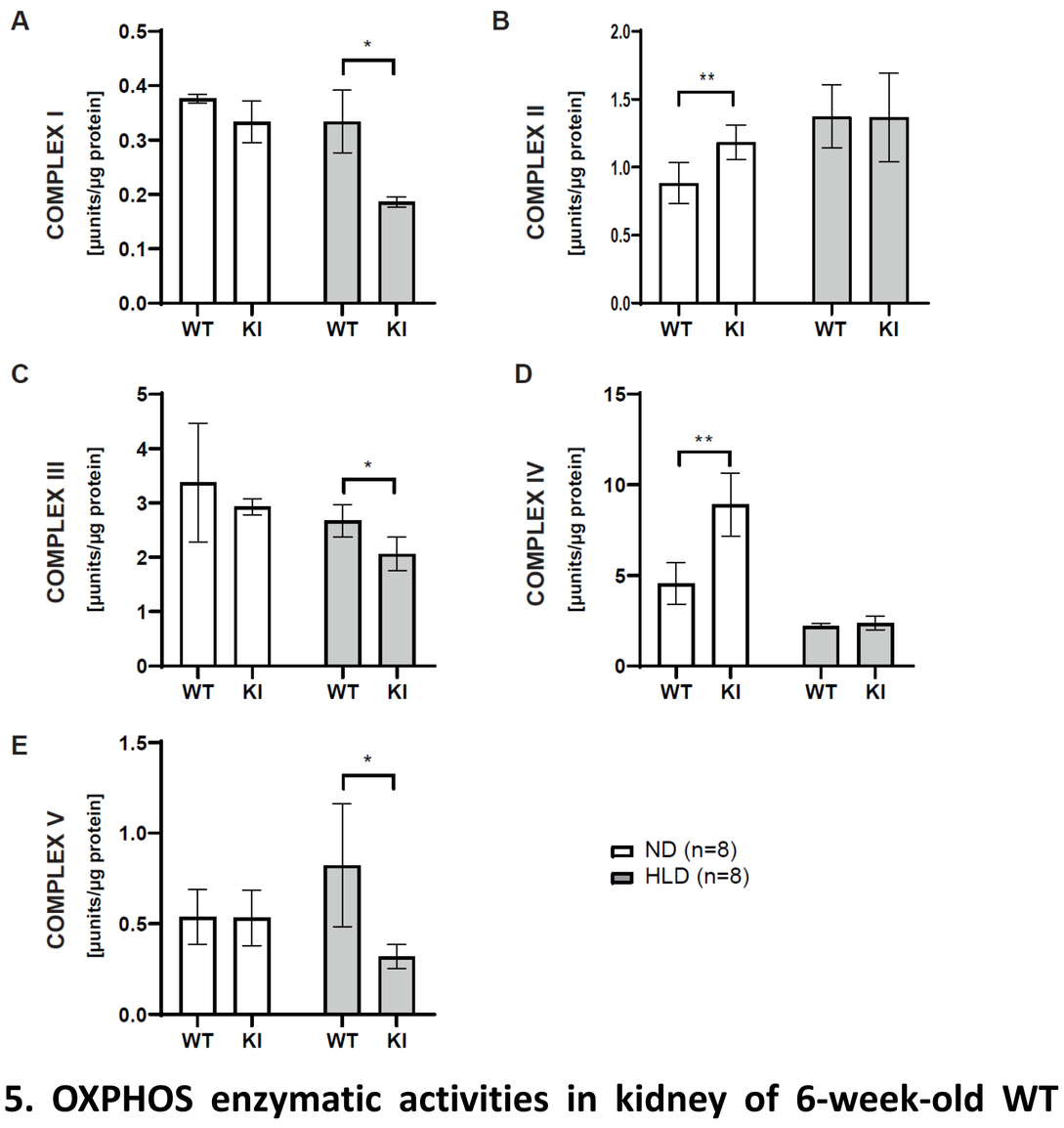

Figure 5. OXPHOS enzymatic activities in kidney of 6-week-old WT and *Gcdh*$^{ki/ki}$ rats under ND and HLD. Quantitative analyses of the enzymatic activities of complex I (**A**), complex II (**B**), complex III (**C**), complex IV (**D**), and complex V (**E**) in kidneys of 6-week-old WT and *Gcdh*$^{ki/ki}$ rats (KI) under ND and HLD (n=8 for each condition). X-axes show genotype, y-axes show µunits/µg protein. Data are shown as mean ± SD; Mann Whitney multiple comparisons: $*p < 0.05$, $**p < 0.01$, after Kruskal Wallis analysis. Enzymatic activity of complex II (Succinate dehydrogenase complex) (**B**), and complex IV (cytochrome c oxidase) (**D**) were found significantly increased in kidneys of *Gcdh*$^{ki/ki}$ (KI) rats under ND. Under HLD, a significant decrease of enzymatic activities in kidneys of *Gcdh*$^{ki/ki}$ (KI) rats was appreciated for complex I (NADH: ubiquinone oxidoreductase) (**A**), complex III (cytochrome c reductase) (**C**) and complex V (ATP synthase) (**E**). Min. n=4 for all conditions.

CHUV

UNIL | Université de Lausanne

Results 3

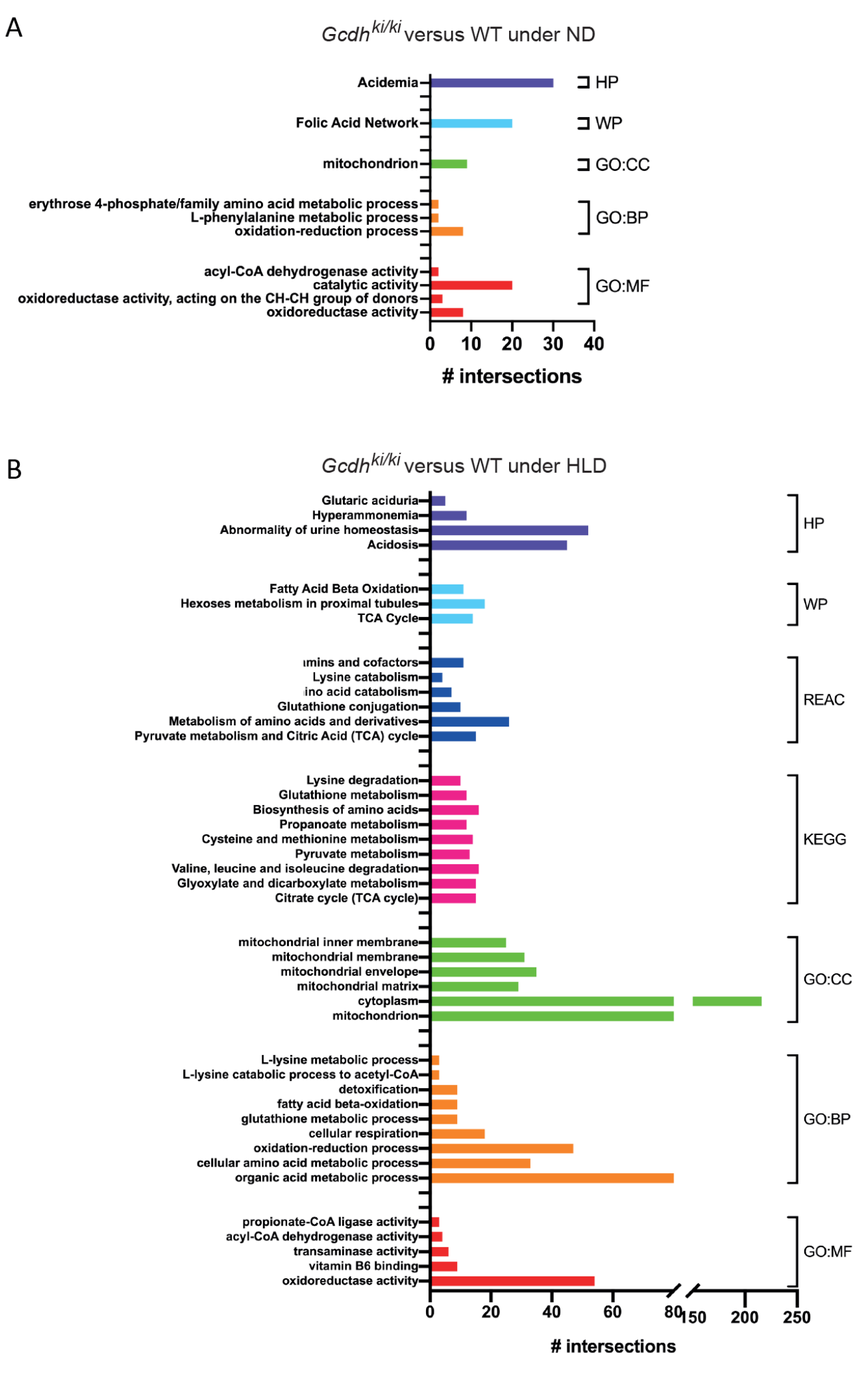

Figure 6. Functional clusterization of *Gcdh*$^{ki/ki}$ rat quantitative differential kidney proteome. Kidney proteome profile of *Gcdh*$^{ki/ki}$ vs WT rats under ND (A) and under HLD (B). The dysregulated kidney proteins in *Gcdh*$^{ki/ki}$ vs WT proteomes were clustered according to HPO (Human Phenotype Ontology), WP (WikiPathways) KEGG (Kyoto Encyclopedia of Genes and Genomes), Gene Ontology (GO) CC (Cellular Component), GO BP (Biological Process) GO MF (Molecular Function) and Reac (Reactome) databases using the g:Profiler software. The pathways graphical enrichment was associated to each cellular pathway (x-axis). Enriched pathways (y-axis) were listed according to enriched values, expressed as numbers of involved proteins (n. intersections) from the *Gcdh*$^{ki/ki}$ proteome datasets.

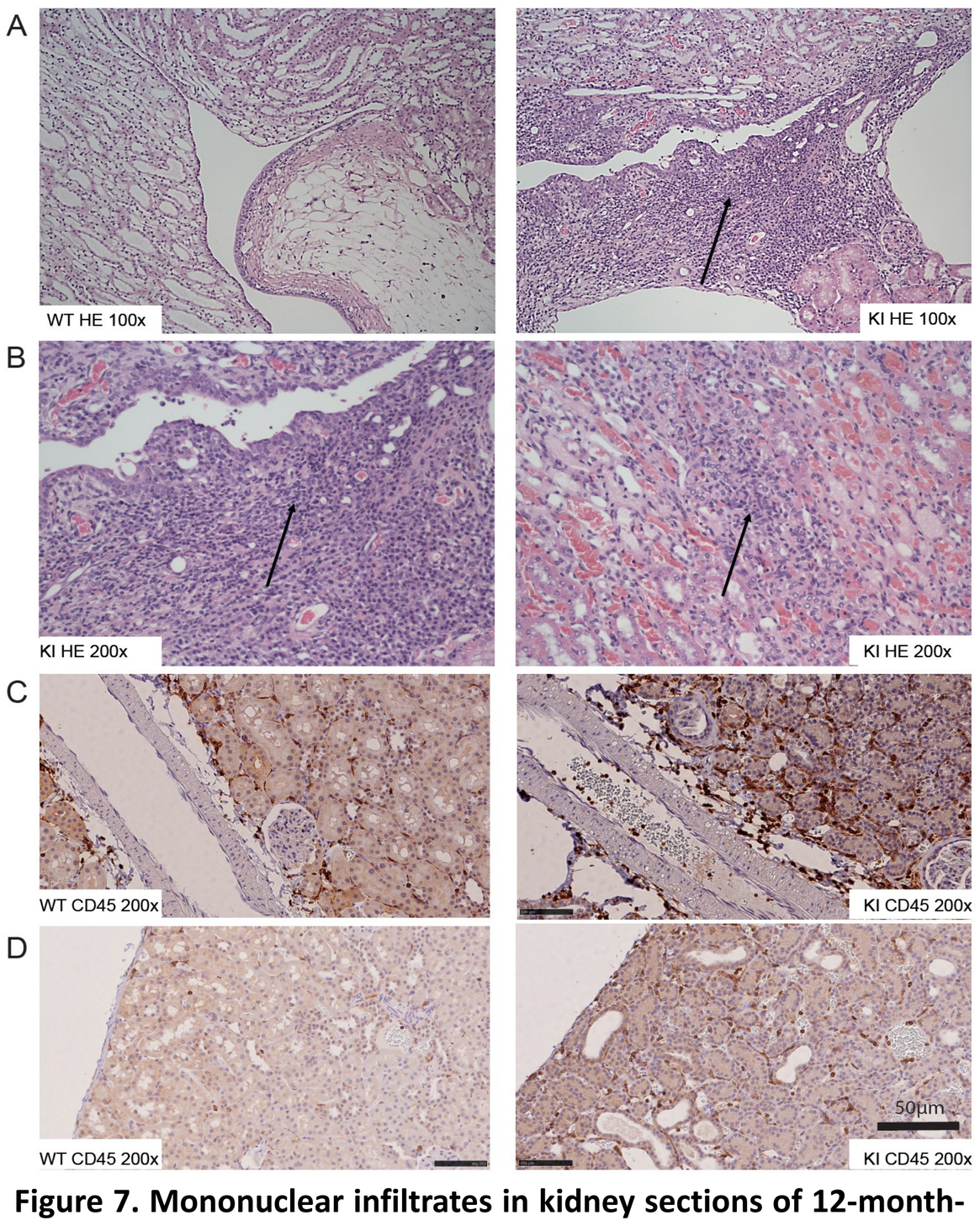

Figure 7. Mononuclear infiltrates in kidney sections of 12-month-old *Gcdh*$^{ki/ki}$ rats. (**A**) HE staining of sagittal kidney sections showed infiltrates (**arrow**) within the renal medulla of 12-month-old *Gcdh*$^{ki/ki}$ (KI) rats (**right**) that were not present in WT rats (**left**). (**B**) HE staining of sagittal kidney sections of 12-month-old *Gcdh*$^{ki/ki}$ (KI) rats at a higher power field revealed infiltrates (**arrows**) in the renal cortex (**left and right**). (**C**) Immunostaining for CD45 on sagittal kidney sections showed mononuclear infiltrates in kidneys of 12-month-old *Gcdh*$^{ki/ki}$ (KI) rats (**right**) around the collector tubules and in the renal cortex (**D**). Scale bar 50 µm. Min. n=4 for all conditions.

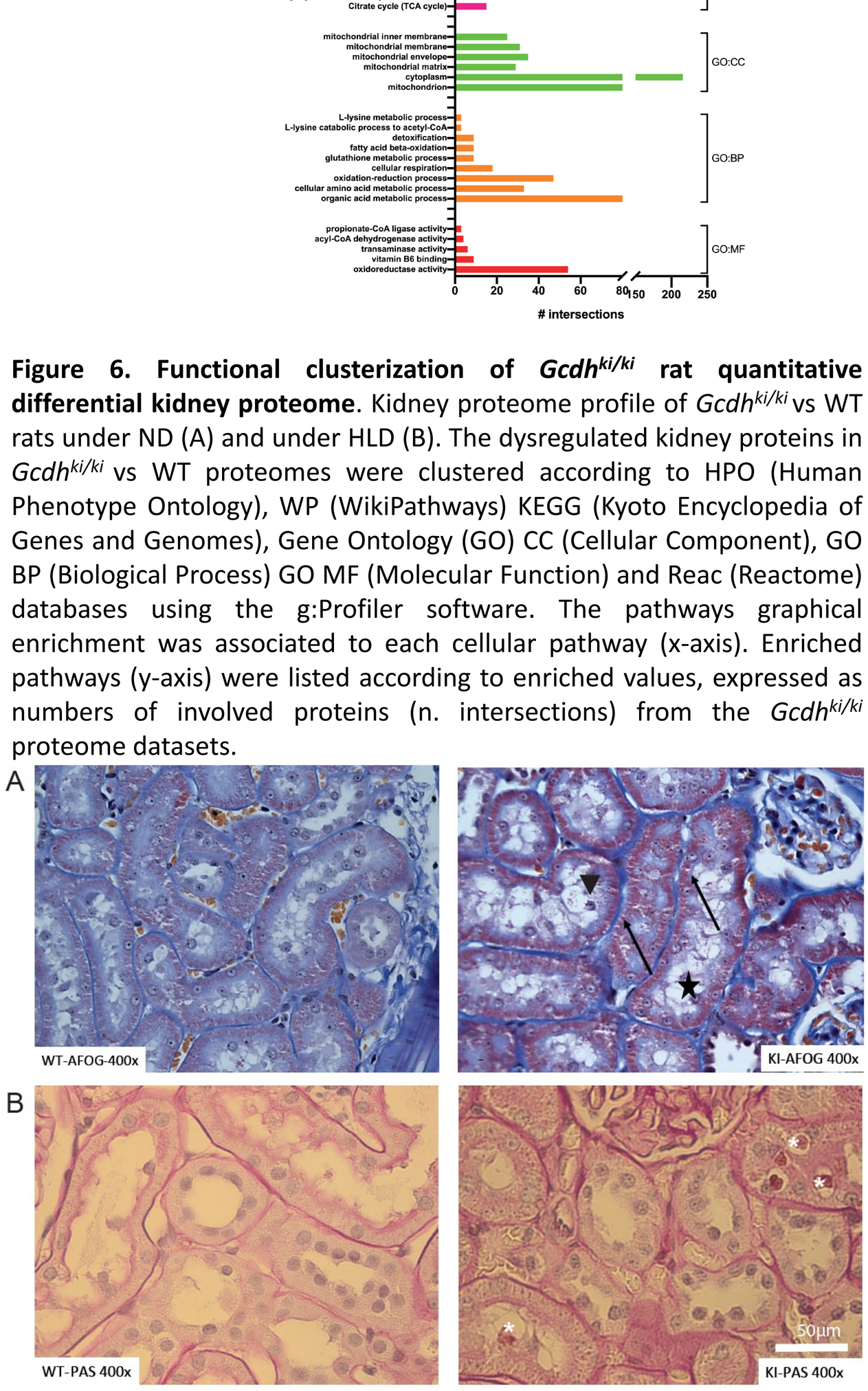

Figure 8. AFOG and PAS stained kidney sections of 12-month-old WT and *Gcdh*$^{ki/ki}$ rats. (**A**) AFOG staining of sagittal kidney sections of 12-month-old WT (**left**) and *Gcdh*$^{ki/ki}$ (KI) rats (**right**). Kidneys of *Gcdh*$^{ki/ki}$ rats (KI) showed an increased amount of proteins (**arrows**) within PT cells and fragmentation of brush border membranes (**star**). Some nuclei of PT cells were observed to be localized in the lumen (**triangle**). Scale bar 50 µm. (**B**) PAS staining of sagittal kidney sections of 12-month-old WT (**left**) and *Gcdh*$^{ki/ki}$ (KI) rats (**right**). Protein accumulation (**asterisks**) was observed in the cytoplasm of PT cells in *Gcdh*$^{ki/ki}$ rats. Scale bar 50 µm. Min. n=4 for all conditions.

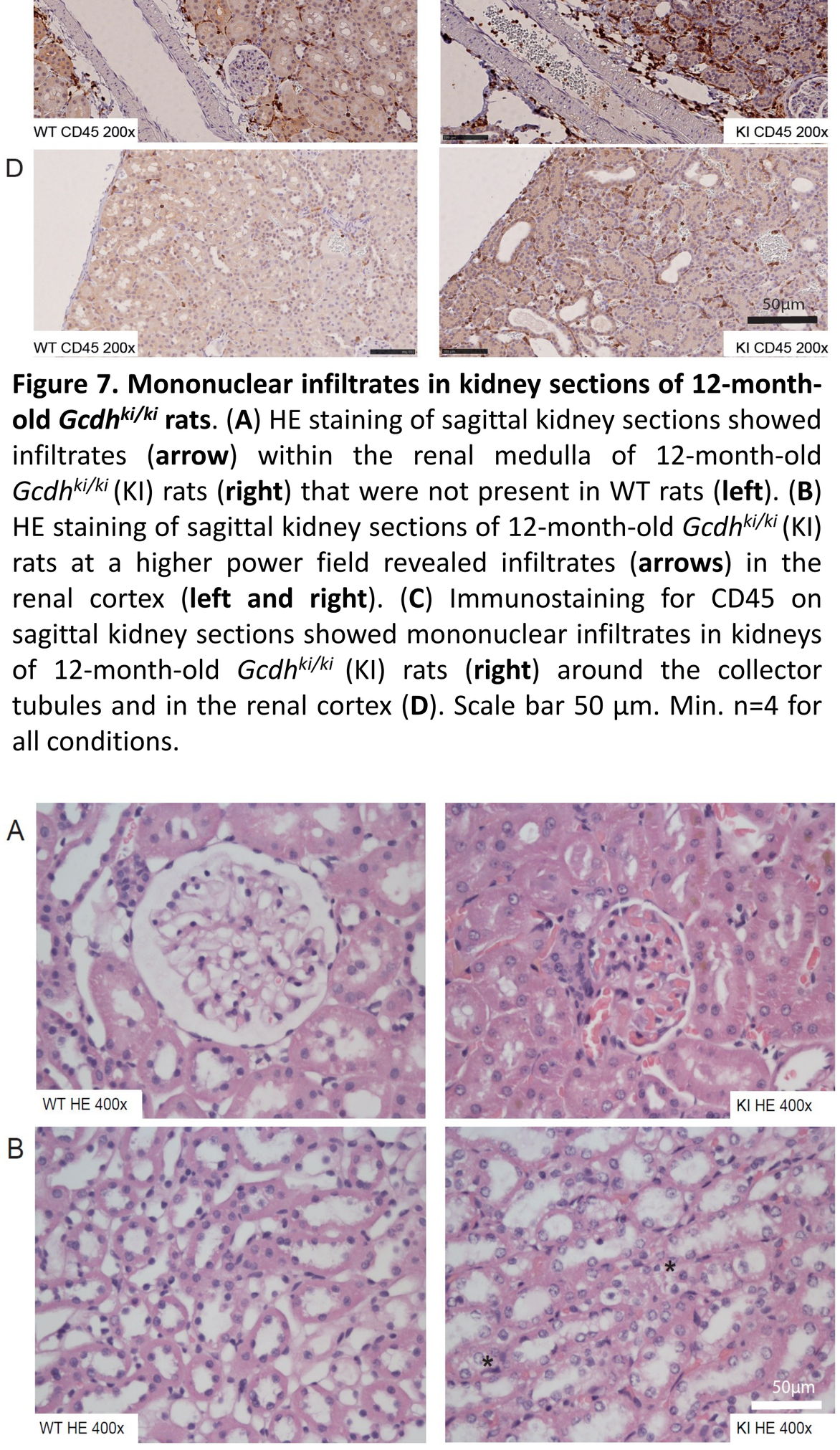

Figure 9. HE stained kidney sections of 12-month-old WT and *Gcdh*$^{ki/ki}$ rats. (A) Glomeruli and PT cells did not show any significant changes between of WT (**left**) and *Gcdh*$^{ki/ki}$ (KI) (**right**) rats. (**B**) Nuclei of distal tubules appeared to be lighter (**asterisks**) in *Gcdh*$^{ki/ki}$ (KI) rats (**right**) compared to WT rats (**left**). Scale bar 50 µM. Min. n=4 for all conditions.

ICIEM 2021

14TH INTERNATIONAL CONGRESS OF INBORN ERRORS OF METABOLISM

21-23 NOVEMBER 2021, SYDNEY, AUSTRALIA

Summary

Acute renal toxicity in GA-I

In young *Gcdh*$^{ki/ki}$ rats exposed to HLD, we observed a GFR decline and biochemical signs of a tubulopathy. Histological analyses revealed lipophilic vacuoles, thinning of apical brush border membranes and increased numbers of mitochondria in proximal tubular (PT) cells. HLD also altered OXPHOS activities and proteome in kidneys of *Gcdh*$^{ki/ki}$ rats.

Chronic renal toxicity in GA-I

In the longitudinal cohort, we showed a progressive GFR decline in *Gcdh*$^{ki/ki}$ rats starting at young adult age and a decline of renal clearance. Histopathological analyses in aged *Gcdh*$^{ki/ki}$ rats revealed tubular dilatation, protein accumulation in PT cells and mononuclear infiltrations.

Conclusions

Our observations confirm that GA-I leads to acute and chronic renal damage. This raises questions on indication for follow-up on kidney function in the aging population of presymptomatically diagnosed GA-I patients and possible therapeutic interventions to avoid renal damage.

Outlook

Renal damage seems to be a late manifestation of GA-I that can significantly alter the quality of life of affected patients. Screening for renal affection in GA-I patients during acute crisis and within the long-term follow-up seems to be indicated. Renal affection is thus a potential new target for therapeutic interventions in GA-I. Future research should focus on the observed pathomechanisms, e.g. by testing antioxidant and/or anti-inflammatory treatments.

Funding

This project was supported by the Swiss National Science Foundation grant number 310030–127497 and by an unrestricted research grant of Nutricia Metabolics (Frankfurt am Main, Germany) given to D. Ballhausen.

FNSNF
Fonds national suisse
Schweizerischer Nationalfonds
Fondo nazionale svizzero
Swiss National Science Foundation

NUTRICIA Metabolics

For further details see our complete article currently in press:

https://doi.org/10.1016/j.ymgme.2021.10.003

CHUV

UNIL | Université de Lausanne